Microscopic level densities

S.Hilaire,
Commissariat à l'Energie Atomique,
Service de Physique Nucléaire,
Boite Postale 12,
91680 Bruyères-le-Châtel, France

Abstract

We present a new combinatorial method to compute exact particle-hole and total level densities in a General Independent Particle Model. This method is first used in the Equidistant Spacing Model framework, and enables us to derive a generalization of the Obložinský formula for particle-hole state densities, that includes correction terms up to arbitrary order. This method is then applied using realistic single particle level schemes obtained from Hartree-Fock-Bogoliubov calculations based on the D1S Gogny force. In this latter case, the collective enhancement of the total level densities is included, and good overall agreement is obtained between our predictions and experimental results for the densities of s-wave neutron resonances. A comparison with the Ignatyuk phenomenological level density parameter formula is presented over a broad energy range. The high energy behavior of our level density parameter is finally discussed in connection with recent results from heavy ion collisions.

1 Introduction

One of the fundamental ingredients for pre-equilibrium and compound nuclear reaction models, is the level density (LD) of excited states. The analytical formulae used to predict such densities have mostly been derived in the Equidistant Spacing Model (ESM). This model is particularly suitable to derive analytical expressions for partial LDs (i.e. with specified numbers of particle-hole (ph) excitations) or for total LDs. For total LDs the few available experimental data enables an adjustment of their theoretical expressions derived in the ESM. In particular, an energy dependent LD parameter is widely adopted to account for properties that cannot be treated in the ESM framework. The only way to deal with microscopic properties of the nucleus, such as shell effects for instance, is a combinatorial calculation of LDs based on realistic single particle level schemes (SPLSs). Although they are time consuming, such combinatorial calculations can be very useful to adjust the various parameters of the generally employed LDs analytical formulae. In view of this, a combinatorial approach has been developed to evaluate both ph and total LDs over a wide energy range and for any spin and parity. The formalism of this approach is presented in Section 2. In Section 3, this method is applied within the ESM framework to derive a new analytical formula for ph LDs. Finally, in Section 4, realistic SPLSs, derived from Hartree-Fock-Bogoliubov (HFB) microscopic calculations based on the D1S Gogny force [1], are used to compute total LDs and discuss their energy variations.

2 Combinatorial formalism

2.1 The intrinsic level densities

In the Independent Particle Model (IPM), the nucleus is represented by two level schemes whose energies are $\varepsilon_1^\pi < \varepsilon_2^\pi < ... < \varepsilon_i^\pi < ...$ for protons and $\varepsilon_1^\nu < \varepsilon_2^\nu < ... < \varepsilon_i^\nu < ...$ for neutrons. The single particle level energies do not depend (i) on the total excitation energy, and (ii) on the number of particles and holes

involved in the excitation of the nucleus. One then defines two SPLSs for each kind of fermion, one for the particles and one for the holes. The holes are as usual the filled single particle levels in the ground state of the nucleus. Denoting by F_π (resp. F_ν) the last filled level in the ground state, one introduces the ph energies

$$\varepsilon_i^1 = \varepsilon^\pi_{F_\pi+i} - \varepsilon^\pi_{F_\pi} \quad \text{for the proton particle levels,}$$

$$\varepsilon_i^2 = \varepsilon^\pi_{F_\pi} - \varepsilon^\pi_{F_\pi-i+1} \quad \text{for the proton hole levels,}$$

$$\varepsilon_i^3 = \varepsilon^\nu_{F_\nu+i} - \varepsilon^\nu_{F_\nu} \quad \text{for the neutron particle levels, and}$$

$$\varepsilon_i^4 = \varepsilon^\nu_{F_\nu} - \varepsilon^\nu_{F_\nu-i+1} \quad \text{for the neutron hole levels.}$$

In the case of axially symmetric nuclei, each level is also defined by its spin projection m_i^k on the symmetry axis, and by its parity π_i^k. The only property to take care of is the fact that the angular momentum contribution for a hole is the opposite of the angular momentum of the state in which the hole is created.

With this notation, the partition function for multiple ph excitations can be written as

$$\mathcal{Z}(x_1, x_2, x_3, x_4, y, t) = \prod_{k=1}^{4} \prod_{i=1}^{I_k} (1 + x_k \pi_i^k \; y^{\varepsilon_i^k} \; t^{m_i^k}).$$

This function is then expanded into a polynomial form of the four variables x_k, and the coefficient $\mathcal{F}_\mathcal{N}(y,t)$ of $x_1^{N_1} x_2^{N_2} x_3^{N_3} x_4^{N_4}$ is developed as in [2] giving

$$\mathcal{F}_\mathcal{N}(y,t) = \prod_{k=1}^{4} \sum_{\{\alpha(N_k)\}} \prod_{j=1}^{N_k} \frac{1}{\alpha_j^k!} \left(\sum_{i=1}^{I_k} \frac{(-1)^{j+1}}{j} (\pi_i^k)^j \; y^{j\varepsilon_i^k} \; t^{jm_i^k} \right)^{\alpha_j^k} , \tag{1}$$

where $\mathcal{N} = (N_1, N_2, N_3, N_4)$, and where the symbol $\sum_{\{\alpha(N_k)\}}$ means summing over all the partitions $(\alpha_1^k, ..., \alpha_{N_k}^k)$ of N_k that fulfill the relation

$$\sum_{i=1}^{N_k} i\, \alpha_i^k = N_k \; .$$

Equation (1) can be expanded as

$$\mathcal{F}_\mathcal{N}(y,t) = \sum_U \sum_M \left(\sum_\pi C_\mathcal{N}(U, M, \pi) \right) y^U t^M \; ,$$

where the coefficients $C_\mathcal{N}(U, M, \pi)$ represent the number of levels resulting from the excitation of N_1 proton particles, N_2 proton holes, N_3 neutron particles and N_4 neutron holes at excitation energy U with an angular momentum M and a parity π.

To compute these coefficients, we assume that energy is a multiple integer of an elementary energy unit ε_0. Thanks to a matricial numerical method, we then obtain the coefficients $C_\mathcal{N}(n, M, \pi)$ representing the sum of all the $C_\mathcal{N}(U, M, \pi)$ values in an energy interval of width ε_0 centered on $U = n\varepsilon_0$. The ph LD is then deduced by summing these coefficients over one MeV width intervals, and the total LD from a summation of all the ph LDs which have the same number of particles and holes. From now on, we call these densities the intrinsic ph and total LDs, respectively.

2.2 Collective effects

We investigate in this Section how to account for collective properties of nuclei, such as vibrations and rotations. We suppose that these collective properties are independent, that is to say there is no coupling between the intrinsic states (i.e. the ph excited states) and the vibrational and rotational effects.

2.2.1 Vibrational states

The independent hypothesis allows us to define a vibrational partition function similar to the boson partition function, which reads

$$\mathcal{Z}_{vib}(y,t) = \prod_{\lambda} \prod_{\mu=-\lambda}^{\lambda} \frac{1}{1 - y^{\varepsilon_{\lambda\mu}}\ t^{\mu}(-1)^{\lambda}}, \tag{2}$$

for a spherical nucleus. In our case, we restrict to quadrupole ($\lambda = 2$) and octupole ($\lambda = 3$) modes, and also account for possible deformation of the nucleus. Therefore, we have to deal with quadrupole β and γ vibrations. That is why we only consider a product over $\mu = -2$, 0 and 2 for $\lambda = 2$ in Eq. (2) for deformed nuclei. Whatever the deformation, in order to compute $\mathcal{Z}_{vib}$ we modify Eq. (2) using the identity

$$\frac{1}{1-x} = 1 + x + x^2 + ... + x^n + ...$$

so that $\mathcal{Z}_{vib}$ can be expanded into a polynomial form. It is therefore possible to compute the number of vibrational states with specified angular momentum and parity in a given energy interval.

Finally, we obtain a vibrational LD that we fold with our intrinsic LD, assuming that any ph excited state can vibrate. We call this new LD the intrinsic vibrational LD, and label it ρ_{iv}.

2.2.2 Deformed nuclei and rotational bands

This part only concerns nuclei which are permanently deformed in their ground state. Such nuclei exhibit rotational band structures clearly observed at low excitation energy. These bands can be described by the knowledge of the head-bands and of the rotational moment of inertia $\mathcal{I}_{\perp}$. Regarding the head-bands, we consider that they are given by each intrinsic vibrational state. We therefore derive what we call the effective level density ρ_{eff} using the relation

$$\begin{aligned}\rho_{eff}(U,J,\pi) = \frac{1}{2} \sum_{K=-J, K\neq 0}^{J} & \rho_{iv}(U - E_{rot}^{J,K}, K, \pi) + \\ & \delta(J\ even)\ \delta(\pi = +)\ \rho_{iv}(U - E_{rot}^{J,0}, 0, \pi) + \\ & \delta(J\ odd)\ \delta(\pi = -)\ \rho_{iv}(U - E_{rot}^{J,0}, 0, \pi)\ ,\end{aligned}$$

where the rotational energy $E_{rot}^{J,K}$ reads

$$E_{rot}^{J,K} = \frac{J(J+1) - K^2}{2\mathcal{I}_{\perp}}.$$

3 New particle-hole LD formula in the ESM

In this Section, we apply the mathematical methods used in [2] to obtain Eq. (1), in order to derive a new ph LD formula in the ESM. This formula is then compared with Obložinský formula and with the exact results yielded by our combinatorial method. A complete derivation of our new formula can be found in Ref. [3].

3.1 The new formula

Starting from the partition function for multiple ph excitations in the ESM, it has been shown [4] that the LD for a given ph configuration $\mathcal{N} = (N_1, N_2, N_3, N_4)$ can be formally expressed in the ESM as

$$\rho_{\mathcal{N}}(U) = \frac{1}{2\pi i} \oint e^{\beta(U-A)} \prod_{k=1}^{4} U_k(\beta)\ D_k(\beta) d\beta\ , \tag{3}$$

where

$$A = \frac{N_1^2 + N_1}{2g_1} + \frac{N_2^2 - N_2}{2g_2} + \frac{N_3^2 + N_3}{2g_3} + \frac{N_4^2 - N_4}{2g_4}\ , \tag{4}$$

$$U_k(\beta) = \prod_{i=1}^{N_k} \left[1 - e^{-\beta \frac{I_k - N_k + i}{g_k}}\right]\ , \tag{5}$$

and

$$D_k(\beta) = \left[\prod_{i=1}^{N_k} \left(1 - e^{-\beta i/g_k}\right)\right]^{-1}\ ,$$

g_i denoting the density of single particle states in the SPLS of type i according to the notation introduced in Section 2.1.

To perform analytically the inverse Laplace transform of Eq.(3), we first replace the subscript i of Eq. (5) by its mean value, and setting $J_k = I_k - 1/2(N_k - 1)$ we obtain

$$U_k(\beta) \approx \sum_{i=0}^{N_k} \binom{N_k}{i} (-1)^i\ e^{-\beta i \frac{J_k}{g_k}}\ . \tag{6}$$

Then, we use the identity

$$1 - e^{-t} = t\ e^{-t/2} \prod_{m=1}^{+\infty} \left[1 + \frac{t^2}{4\pi^2 m^2}\right]\ .$$

throughout, to obtain for D_k the relation

$$D_k(\beta) = \frac{e^{\beta N(N+1)/4}}{N! \beta^N} \left[1 + \sum_{k=1}^{+\infty} C_{2k}(N)\ \beta^{2k}\right]\ , \tag{7}$$

with

$$C_{2k}(N) = \sum_{\{\alpha(k)\}} \prod_{i=1}^{k} \frac{1}{\alpha_i!} \left[\frac{(-1)^i}{i\, 4^i \pi^{2i}} \sum_{m=1}^{+\infty} \frac{1}{m^{2i}} \sum_{j=1}^{N} j^{2i}\right]^{\alpha_i}\ , \tag{8}$$

the symbol $\sum_{\{\alpha(k)\}}$ denoting the summation over all the combinations $(\alpha_1, ..., \alpha_N)$ that obey

$$\alpha_1 + 2\,\alpha_2 + ... + k\,\alpha_k = k\ .$$

Inserting Eqs. (6) and (7) into Eq. (3), and performing the inverse Laplace transform finally leads to

$$\rho_{\mathcal{N}}(U) = G \sum_{i=0}^{N_1} \sum_{j=0}^{N_2} \sum_{k=0}^{N_3} \sum_{l=0}^{N_4} K_{ijkl}\ \Theta(U_{ijkl} - B) \left[\sum_{m=0}^{E\left[\frac{M-1}{2}\right]} E_{2m}^{\mathcal{N}} \frac{U_{ijkl}^{(M-2m-1)}}{(M-2m-1)!}\right]\ , \tag{9}$$

where Θ denotes the Heaviside function,

$$G = \frac{{g_1}^{N_1} {g_2}^{N_2} {g_3}^{N_3} {g_4}^{N_4}}{N_1!\, N_2!\, N_3!\, N_4!} \ ,$$

$$K_{ijkl} = (-1)^{i+j+k+l} \binom{N_1}{i} \binom{N_2}{j} \binom{N_3}{k} \binom{N_4}{l} \ ,$$

$$U_{ijkl} = U - A + B - E_{ijkl} \ ,$$

with the Pauli energy A defined in Eq. (4),

$$B = \frac{N_1^2+N_1}{4g_1} + \frac{N_2^2+N_2}{4g_2} + \frac{N_3^2+N_3}{4g_3} + \frac{N_4^2+N_4}{4g_4} \ ,$$

$$E_{ijkl} = i\,\frac{J_1}{g_1} + j\,\frac{J_2}{g_2} + k\,\frac{J_3}{g_3} + l\,\frac{J_4}{g_4},$$

where the J_n's have been introduced in Eq. (6),

$$E_{2m}^{\mathcal{N}} = \sum_{i=0}^{m} D_{2m-2i}(N_1, N_2)\ D_{2i}(N_3, N_4), \qquad (E_0^{\mathcal{N}} = 1) \ ,$$

and

$$D_{2k}(N_i, N_j) = \sum_{l=0}^{k} \frac{C_{2k-2l}(N_i)\ C_{2l}(N_j)}{{g_i}^{2k-2l}\ {g_j}^{2l}},$$

with the coefficients $C_{2k}(N)$ defined in Eq. (8), and with

$$M = N_1 + N_2 + N_3 + N_4 \ .$$

The complicated formula (9) reduces to the analytical formula derived in [4] if one neglects the coefficients $E_{2m}^{\mathcal{N}}$ for $m \geq 1$. Regarding these coefficients, they have been first derived up to $m = 2$ in [5] to improve the well known Williams formula [6], and we have given them in a closed form to use them all.

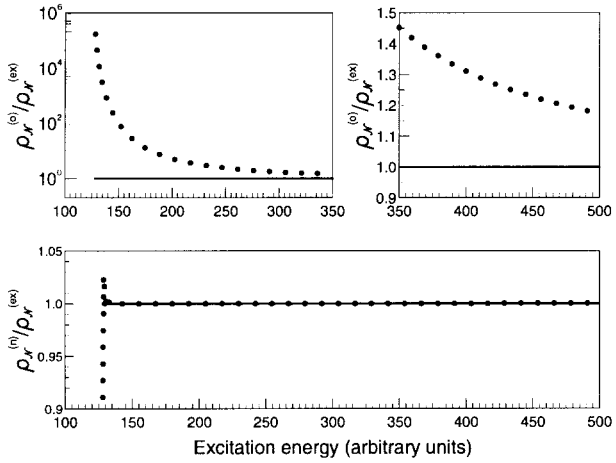

Figure 1: *Comparison between exact calculations and analytical formulae predictions for the proton-neutron configuration* $\mathcal{N} = (8,8,8,8)$ *in* ^{208}Pb. *The solid lines represent unity and the closed circles are the ratios* $\rho_{\mathcal{N}}^{(o)}/\rho_{\mathcal{N}}^{(ex)}$ *(top) and* $\rho_{\mathcal{N}}^{(n)}/\rho_{\mathcal{N}}^{(ex)}$ *(bottom).*

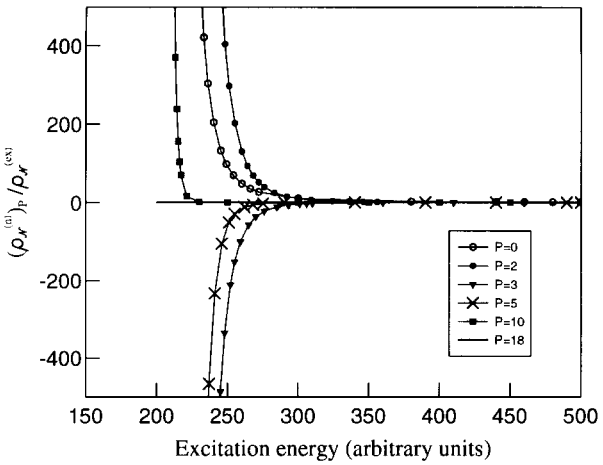

Figure 2: *Comparison between exact calculations and the truncated state density* $\left(\rho_{\mathcal{N}}^{(2)}\right)_P$ *predictions for various values of* P *in the case of the proton-neutron configuration* $\mathcal{N} = (10, 10, 10, 10)$ *in* ^{208}Pb.

3.2 Results and discussion

We now compare the results obtained using our new ph LD formula (labeled $\rho_{\mathcal{N}}^{(n)}$) and those given by Obložinský (labeled $\rho_{\mathcal{N}}^{(o)}$), to the exact results (labeled $\rho_{\mathcal{N}}^{(ex)}$) obtained using our combinatorial approach. For simplicity, we set $g_1 = g_2 = g_3 = g_4 = g_0$ and use an arbitrary energy unit equal to g_0^{-1}. Since the LDs may take either very low or very high values, we plot the ratios between each analytical formula and the exact values.

In Fig. 1, the proton-neutron configuration $\mathcal{N} = (8, 8, 8, 8)$ is shown for ^{208}Pb. On the left and right upper panels we plot $\rho_{\mathcal{N}}^{(o)}/\rho_{\mathcal{N}}^{(ex)}$, and on the lower panel $\rho_{\mathcal{N}}^{(n)}/\rho_{\mathcal{N}}^{(ex)}$. As can be seen, the effect of the coefficients $E_{2m}^{\mathcal{N}}$ is much more important at low energy (i.e. near the Pauli energy) than it is at high energy. Over the whole energy range, the agreement of our new formula with the exact calculation is excellent, even if a little deviation from unity appears near the Pauli energy. However, this deviation is very weak compared to what it is without the corrections we have introduced.

To study further the effects of the coefficients $E_{2m}^{\mathcal{N}}$ and to see whether it is possible to limit the number of $E_{2m}^{\mathcal{N}}$ values to be used in actual calculations, we define the truncated form of Eq. (9) as

$$\left(\rho_{\mathcal{N}}^{(n)}\right)_P(U) = G \sum_{i=0}^{N_1}\sum_{j=0}^{N_2}\sum_{k=0}^{N_3}\sum_{l=0}^{N_4} K_{ijkl}\,\Theta(U_{ijkl} - B)\left[\sum_{m=0}^{P} E_{2m}^{\mathcal{N}}\,\frac{U_{ijkl}^{(M-2m-1)}}{(M-2m-1)!}\right], \tag{10}$$

and represent in Fig. 2 the results obtained with different P values in the configuration $\mathcal{N} = (10, 10, 10, 10)$ for ^{208}Pb. We observe that (i) an even value of P must be imposed (otherwise the LD might become negative), and (ii) that all the coefficients $E_{2m}^{\mathcal{N}}$ must be included to get a good agreement over the whole energy range, since $\left(\rho_{\mathcal{N}}^{(n)}\right)_0$ may be a better approximation at low excitation energy than $\left(\rho_{\mathcal{N}}^{(n)}\right)_2$ for instance.

4 Results in a GIPM

In this Section we study the results given by our combinatorial approach using realistic SPLSs obtained from Hartree-Fock-Bogoliubov calculations based on the D1S Gogny force. We first study the densities of s-wave neutron resonances (DNR) for various even-even nuclei covering the entire mass range. Then we study the energy dependency of the LD parameter a obtained by fitting our combinatorial results with the well known expression for LDs

$$\rho(U) = \frac{\sqrt{\pi}}{12} \frac{e^{2\sqrt{a(U-\Delta)}}}{a^{1/4}(U-\Delta)^{5/4}}.$$

We finally look at the asymptotic value of a to see whether it behaves like $A/8$ or rather like $A/13$, a value which has been recently suggested [7, 8, 9, 10, 11].

4.1 The combinatorial DNR

We now compare the tabulated DNR of [12] with those obtained from our combinatorial approach. The vibrational states are taken into account using the vibrational partition function (2) with the energies $\varepsilon_{\lambda\mu}$ of [13]. For the rotational moment of inertia, we use the rigid-body moment of inertia calculated like in [12]. In Fig. 3 (a), we plot the results obtained directly from our combinatorial calculations, while Fig. 3 (b) shows the results corrected to take into account the pairing energy [1]. As can be seen, the agreement between microscopic and experimental DNR is better when a pairing correction is included. Indeed, in Fig. 3 (a), the DNR experimental values are strongly underestimated for the $A < 150$ mass region, while they are quite well reproduced in Fig. 3 (b). However, in Fig. 3 (b), some discrepancies not seen in Fig. 3 (a) can yet be observed in the rare earth and actinide regions. These might be due to vibrational states which have not been taken into account, such as hexadecapole vibrational modes or isovectors modes. If a proper treatment of such modes were made, the underestimation observed in the $A < 150$ region in Fig. 3 (a) would cover the entire mass range, whereas a better agreement would be obtained in Fig. 3 (b) in the rare earth and actinide regions.

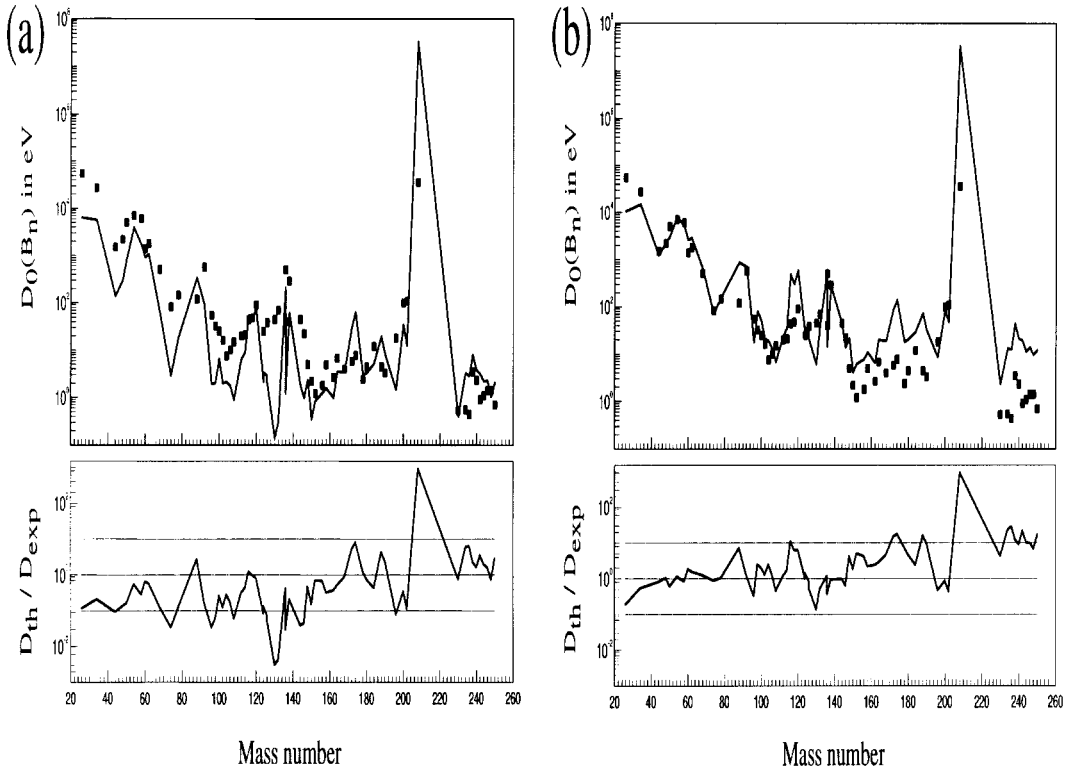

Figure 3: *Comparison between experimental DNR (D_{exp}) from Iljinov et al. [12] and theoretical predictions (D_{th}) based on our combinatorial approach without any pairing correction (a) and with a pairing correction (b). The solid boxes show D_{exp} and the solid line D_{th}.*

[1] The pairing correction is obtained by shifting the intrinsic ph LDs of the energy Δ_n, Δ_p or $\Delta_n + \Delta_p$. when the ph configuration is a neutron, proton, or proton-neutron configuration, respectively.

4.2 Energy dependency of the LD parameter a

We now study the LD parameter for various energies as a function of the mass number. The results are compared with the phenomenological description given by Ignatyuk [14]

$$a(N,Z,U) = \tilde{a}(A)\left(1 + \frac{\delta W(N,Z) f(U-\Delta)}{U-\Delta}\right) , \tag{11}$$

where $f(U)$ is an ad hoc damping function used to describe the known weakening of shell effects with increasing excitation energy [15], $\delta W(N,Z)$ is the shell correction to the mass formula [16, 17, 18] calculated in our case using the Strutinsky method [16], and $\tilde{a}$ is the asymptotic value of a.

To do this comparison, we do not include the vibrational states since it is known that they vanish with increasing excitation energy. We therefore only include the rotational effects. Moreover, we consider two kinds of LD parameter, namely the intrinsic a_{int} deduced from the combinatorial calculation without inclusion of the rotational effects, and the effective LD parameter a_{eff} obtained when rotational effects are included. As can be seen in Fig. 4, shell effects are clearly observed and strongly correlated with the shell correction energy $\delta W(N,Z)$. What is remarkable, is the fact that the intrinsic LD parameter follows the functional form (11) since it increases with increasing excitation energy when $\delta W(N,Z)$ is negative, and decreases when $\delta W(N,Z)$ is positive, whereas a_{eff} does not. This is a consequence of the rotational effects. Moreover, one can also observe that the high energy value of both a_{int} and a_{eff} behaves like $A/13$ and not like $A/8$. In fact, the $A/8$ behavior is only obtained at low energy when vibrational states are included as shown in Fig. 5, where the calculations made in Section 4.1 have been used to deduce a_{eff} for an excitation energy equal to the neutron binding energy.

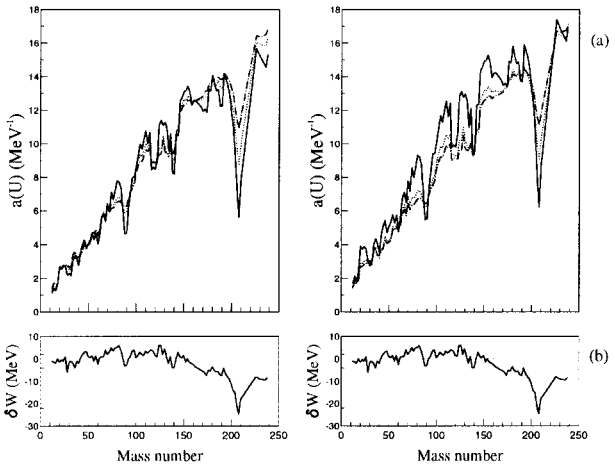

Figure 4: *(a) Calculated level density parameter as a function of the mass number for various energies. On the left is shown a_{int} and on the right is shown a_{eff}. In both cases, the full line is for $U = 15$ MeV, the dotted line for $U = 45$ MeV and the dash-dotted line for $U = 90$ MeV. (b) Shell corrections. Single particle levels are from present HFB calculations.*

4.3 Mass dependency of the LD parameter

We now study the mass dependency of the intrinsic LD parameter. To do this we have calculated the total LDs for about 400 even-even nuclei. We show in Fig. 6 the results for two excitation energies, namely $U = 15$ MeV and $U = 90$ MeV. As can be seen, when the excitation energy is low there is a important dispersion of the level density parameters values, while for high excitation energy, the dispersion reduces and the level density values seem to follow a straight line. One can then conclude that the asymptotic level density parameter is not depending on the number of protons and neutrons, but simply on the mass number as predicted by the theory. Moreover, the $A/13$ behavior is evident except for the lowest masses

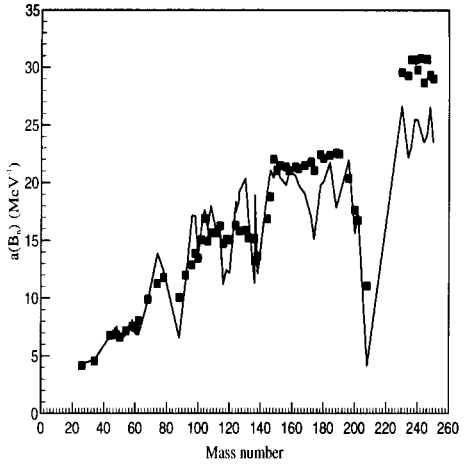

Figure 5: *Calculated level density parameter at the neutron binding energy (solid line) compared with the experimental values tabulated in [12] (solid boxes). Single particle levels are from present HFB calculations.*

where the $A/8$ behavior seems more reasonable. Also, one can still observe important shell effects in the lead region, although it is generally assumed that they vanish above 50 MeV.

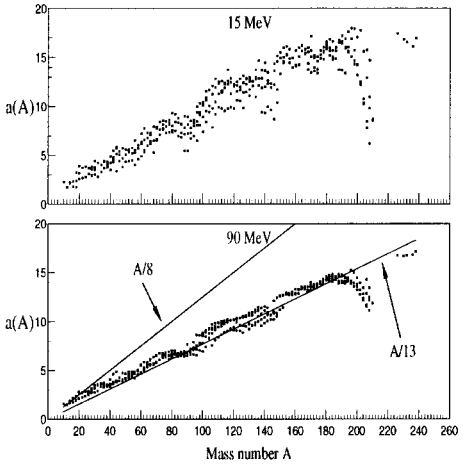

Figure 6: *Level density parameter for various nuclei as function of the mass number A for low and high excitation energy.*

5 Conclusion

We have performed microscopic level densities calculations, both for the ESM and for realistic SPLs obtained from HFB method based on the D1S Gogny force For the ESM, we have generalized the analytical formula of Obložinský. We have also shown that it is possible to reproduce quite well the experimental DNR with our combinatorial method, provided that the vibrational and rotational effetcs are correctly accounted for. We feel therefore confident in the predictive character of our microscopic approach when no experimental data are available. We have also shown that the functional form of the Ignatyuk formula was correct to describe the intrinsic level density parameter energy dependency. However, this functional form needs to be modified since (i) the asymptotic level density behavior is $A/13$ and not $A/8$, and (ii) because shell effects do not vanish as fast as predicted. Our microscopic approach is also very interesting

since it can be applied for superdeformed or isomeric nuclei, and also in the case of transitional states in fission studies. Moreover, it enables us to deal with both particle-hole and total level densities within the same model, which would be very useful when studying pre-equilibrium reactions.

6 Aknowledgments

The author is indebted to Ch. Lagrange who has inspired this work. He also wishes to thank J. F. Berger and J. P. Delaroche for fruitful discussions. He feels particularly grateful to M. Girod for providing him all the HFB+D1S single particle level schemes used in the present work.

References

[1] J. F. Berger, M. Girod and D. Gogny, Comp. Phys. Comm. **63**, 365 (1991).

[2] J. F. Berger and M. Martinot, Nucl. Phys. **A226**, 391 (1974).

[3] S. Hilaire, J. P. Delaroche and A. J. Koning, submitted to Phys. Rev. C.

[4] P. Obložinský, Nucl. Phys. **A453**, 127 (1986).

[5] A. Anzaldo Meneses, Z. Phys. **A353**, 295 (1995).

[6] F. C. Williams, Nucl. Phys. **A116**, 231 (1971).

[7] G. Nebbia et al., Phys. Lett. **B176** (1986) 20.

[8] D. Fabris et al., Phys. Rev. **C50** (1994) R1261.

[9] K. Hagel et al., Nucl. Phys. **A486** (1988) 429.

[10] M. Gonin et al., Phys. Lett. **B217** (1989) 406.

[11] C. Gregoire et al., Nucl. Phys. **A530** (1991) 94.

[12] A. S. Iljinov et al. , Nucl. Phys. **A543**, 517 (1992).

[13] C. M. Lederer and V. S. Shirley, Tables of Isotopes, Wiley, N.Y. (1978).

[14] A. V. Ignatyuk et al. , Sov. J. Nucl. Phys, **21** 255 (1975).

[15] J. R. Huizenga and L. G. Moretto, Ann. Rev. Nucl. Sci. **22**, 472 (1972).

[16] V. M. Strutinsky, Nucl. Phys. **A122**, 1 (1968).

[17] W. D. Myers and W. J. Swiatecki, Ark. Fys. **36**, 343 (1967).

[18] J. W. Truran et al. , Proc. Int. Conf. on The Properties of Nuclei, Leisin, 1970, vol. 1, p. 275.